Breakdown Resistance Analysis of Traction Motor Winding Insulation under Thermal Ageing

K. N. Gyftakis, P. A. Panagiotou, N. Lophitis
School of CEM and Research Centre for Mobility and Transport, Coventry University
Coventry, UK
k.n.gyftakis@ieee.org

D. A. Howey and M. D. McCulloch
Department of Engineering Science
University of Oxford
Oxford, UK

***Abstract*—Stator inter-turn faults are among the most important electric motor failures as they progress fast and lead to catastrophic motor breakdowns. Inter-turn faults are caused due to the windings' insulation degradation. The main stress which deteriorates the insulation is the thermal one. Proper understanding of how this stress influences the electrical properties of insulation over time may lead to reliable prognosis and estimation of the motor's remaining useful life. In transport applications where reliability and safety come first it is a critical issue. In this paper, extensive experimental testing and statistical analysis of thin film insulation for traction motor windings has been performed under fixed thermal stress. The results indicate that for high thermal stress the electrical properties of the insulation material present a non-monotonic behavior thus proving the well-known and established Arrhenius law inadequate for modelling this type of problems and estimating the remaining useful life of thin film insulation materials.**

Keywords—breakdown voltage; degradation; insulation; electric motor; prognosis

I. INTRODUCTION

Electric motors operating in electric vehicle applications are subjected to intense stresses [1]. Although usually powerful in terms of efficiency and output power, traction electric motors may indeed experience faults of different origin and severity, which may lead to motor breakdown and unsafe drive cycle [2]. So, condition monitoring of the electric motor is required. In general, condition monitoring constitutes of two different scientific areas namely the fault diagnosis [3] and the fault prognosis [4]. The former deals with the prompt detection of an existing fault at incipient levels while the latter focuses on estimation of the motor's remaining useful life.

Among the different failure types, the stator inter-turn fault is one of the most severe. This is due to its fast evolution from low severity level to catastrophic motor breakdown. A past study on induction motors showed that this evolution may happen in less than one minute [5]. So, it becomes evident that for this fault type, prognosis may be more valuable because the time offered for fault diagnosis and appropriate correcting actions may not be enough. It is not to be forgotten that the main challenge of stator inter-turn fault detection is also its discrimination from the supply imbalance [6]-[7]. In spite of the aforementioned, the fault diagnosis of stator inter-turn faults is challenging and invites many research efforts worldwide [8]-[9].

Practically, the stator inter-turn fault will happen due to the insulation ageing. This means that many ageing factors, which can be found in the literature as TEAM (Thermal, Electrical, Ambient and Mechanical) [10] will progressively lead to degradation of the windings insulation. Eventually, the insulation will lose its critical dielectric properties and allow for an electrical connection and consequently a current to flow between neighbouring conductors resulting to an inter-turn short circuit fault. Modelling the multi-physical character of the degradation of the insulation material may allow for the accurate prediction of failures as well as estimation of the motor's remaining useful life.

In the literature many significant contributions can be acknowledged. In [11] it was found that a failed induction motor had experienced a significant resin weight loss. In addition, it was found in [12] that after the initial ageing cycles, there was a shift of the dissipation factor and the capacitance at all voltage levels toward lower losses and capacitances because of the drying out and post curing of the insulation. Moreover, a new life span model was developed in [13], which presents an original relationship between the insulation life span and the stress parameters with the application of the design of experiments (DoE) methodology. Furthermore, a continuous monitoring method is presented in [14], based on monitoring frequency changes of the current in inverter-fed induction motors, The impact of the parasitic capacitances of the inverter on the reliability of the method was shown in [15]. In [16], the authors experienced a 20% capacitance drop of their tested windings after five thermal cycles. Additionally, an equivalent circuit model of induction motors was presented in [17] to account for thermal stress. In [18]-[19] the impact of thermal degradation on the dielectric properties of thin film insulation material used for windings of traction electric motors has been studied. Finally, the authors of [20] compare different methods for evaluating the relative importance of variables involved in insulation lifespan models using twisted pairs under different stress constraints.

The main challenge, for reliable prognosis, appears to be the inherent difficulty of separating the different physical mechanisms, as well as their independent impact on the

insulation ageing. For example, testing insulation under electrical stress means flow of current in the tested winding and production of heat. Heat automatically means thermal degradation co-existing with the electrical one. Moreover, thermal cycling means different mechanical expansion rates between different materials resulting to co-existence of mechanical stress with the thermal one. So, it becomes clear that an appropriate research plan would primarily require understanding and modelling of fixed thermal stress. A second step would require of thermal cycling, where it would be possible to discriminate the impact of mechanical expansion rates from thermal ageing. Electrical testing should also be done independently to make it possible to subtract the impact of thermal stress and mechanical expansion stress and isolate the electrical one. Following a procedure like the above it will be possible to model the insulation degradation accurately and consisting of each independent ageing mechanism together.

So, in this work the impact of fixed thermal stress on the resistance of winding insulation material is investigated. A population of samples has been aged under different temperatures and for different time periods. The samples are subjected to electrical breakdown testing to extract valuable information on their remaining useful life. The results show that the well-known Arrhenius law [22]-[23] is not capable of describing the ageing mechanism and that the actual degradation is much more complex. However, very useful conclusions are made as to the prediction of the winding insulation remaining useful life, as well as its characteristics at different stages of the thermal degradation procedure.

II. Experimental Procedure

The work focuses on the analysis and understanding of the thermal degradation of windings insulation coating material. For this purpose, rectangular copper wire with Class H insulation has been used. The cross section dimensions of the wire are 15.24 mm wide by 2.54 mm thick with an insulation coating thickness of approximately 60 microns. The insulation coating consists of two layers, an inner made of polyester-imide (PEI) and an outer of polyamide-imide (PAI). A population of samples was prepared by cutting the wire in bars of 300mm length. The samples were grouped in teams of 6 bars each. Each team was aged under a specific temperature and for a specific time period thus its samples are expected to express similar degradation characteristics and allow for reliable statistical analysis. Four identical ovens were set up with fixed temperatures 200°C, 215°C, 230°C and 245°C to host the samples. One of the ovens containing samples is shown in Fig. 1. A total of 30 samples was introduced in each oven. After accelerated thermal ageing periods of 100hours, 200hours, 400hours, 800hours and 1600hours a team of 6 bars was extracted from each oven. Finally, it is important to note that a population of 11 unaged samples was also prepared for comparison purposes.

The samples were then prepared for breakdown voltage testing under high voltage. The breakdown voltage measurement was carried out using the conductive tape approach as defined in the standard IEC 60851-5. Four conductive aluminium tape stripes were placed on the surface of each bar as shown in Fig. 2-a. Then the sample is placed in a dielectric protection case to avoid any unwanted leakage discharges. Finally, the high voltage electrodes are connected. The negative electrode is connected to one aluminium stripe end at a time, while the positive is electrically connected to the copper inside at one end of the bar (Fig. 1-c). The measurements were conducted using a CA6555 Chauvin-Arnoux 15kV Megohmmeter. The produced voltage ramp is according to Fig. 1-d. The voltage is fixed at 500V for 1 minute. Then it progressively increases linearly up to 15kV in 13 minutes. Finally, the voltage is fixed at 15kV for 1 minute. The instrument has been programmed under Early Breakdown Voltage (EBV) mode; when the current through the electrodes increases rapidly and reaches 0.2mA then the supplied voltage is immediately shut down. In this way, no catastrophic damage is inflicted upon the insulation samples. For safety reasons, the Megohmmeter was connected via optic cable and controlled by a remote PC.

a)

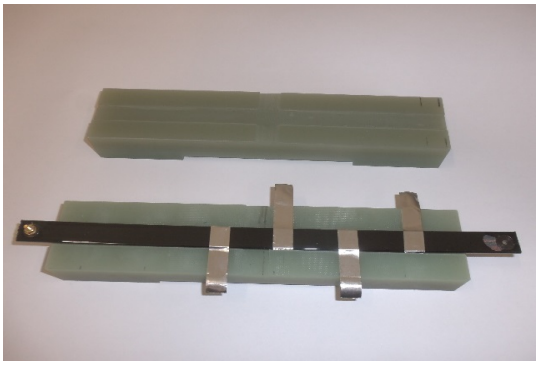

b)

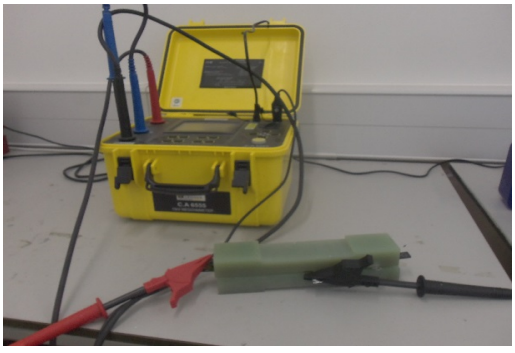

c)

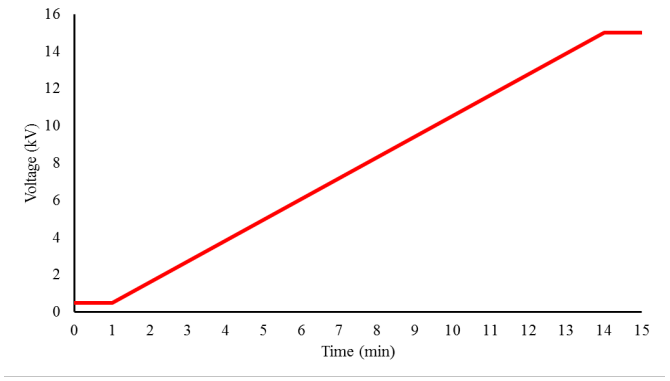

d)

Fig. 1. Experimental setup: a) samples in the oven, b) dielectric case and a sample with aluminium tapes, c) Meghommeter attached to a tested sample and d) applied voltage ramp.

Three consecutive measurements took place on every tested point. This approach was followed after observing that one measurement alone was not enough to indicate the EBV accurately in samples of low degradation levels. A second measurement on the same tested insulation point led to significantly higher EBV, while a third one slightly higher. However more than three repetitions were avoided due to the significantly increased time required for every test and because the accuracy was at acceptable levels. Some results from the experimental procedure can be seen in Fig. 2 and Fig. 3 for tested points under 200°C, 100 hours and 230°C, 800 hours respectively. The blue line represents the voltage ramp while the red line the instantaneous resistance. It is evident that the tested sample point at 230°C, 800 hours has a significantly lower resistance at breakdown than the point at 200°C, 100 hours.

Before running the testing procedure all samples were closely inspected for testing appropriateness and reliability. For example, one point on one of the unaged samples was found to be slightly scratched and so it was left out of our testing procedure. So, in the end a total population of 43 out of expected 44 tested points representing unaged insulation state was considered.

Similarly, any points on the aged samples considered unreliable/damaged after the inspection, were excluded from the analysis. Specifically, some samples at high temperatures and for long degradation periods did not survive the ageing procedure and were catastrophically damaged thus not tested at all. For example, more than half samples were catastrophically damaged under 230°C after 1600 hours. No samples survived this ageing period under 245°C. Finally, two samples were catastrophically damaged after 800 hours and under 245°C. The population of tested points for every degradation state group is shown in Table I. The table cells representing groups with reduced sample population due to catastrophic deterioration of the insulation material are shaded in yellow colour.

TABLE I. POPULATIONS OF TESTED SAMPLE POINTS PER DEGRADATION LEVEL GROUP

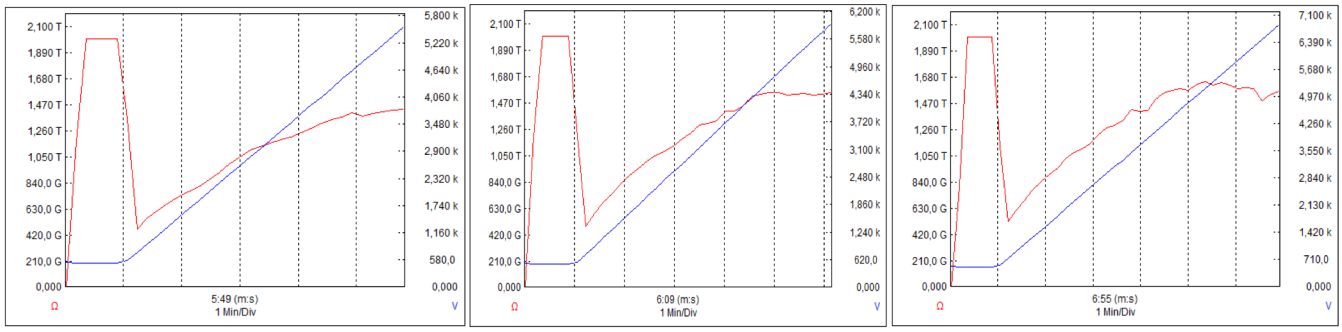

a) b) c)

Fig. 2. Three consecutive EBV measurements on a tested point degraded at 200°C for 100 hours.

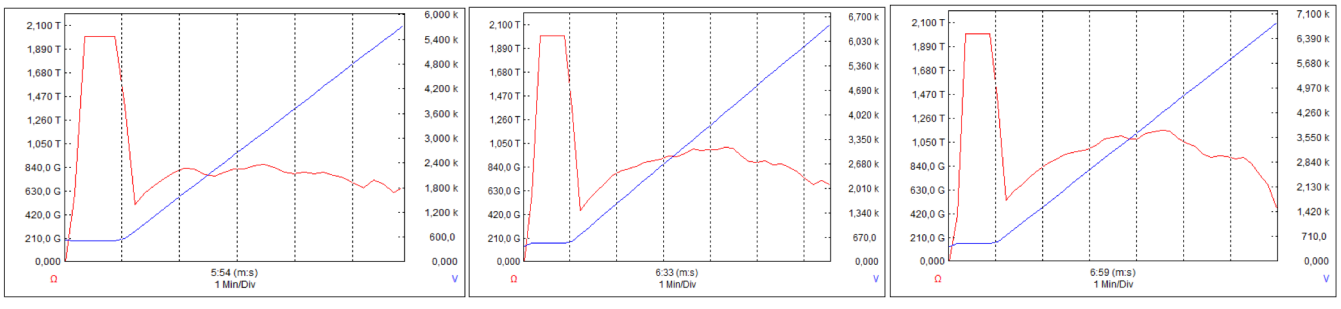

a) b) c)

Fig. 3. Three consecutive EBV measurements on a tested point degraded at 230°C for 800 hours.

Temperature (°C)	100 hours	200 hours	400 hours	800 hours	1600 hours
200	24	23	23	22	23
215	23	23	24	24	23
230	24	24	22	24	10
245	24	24	24	16	0

III. Results and Analysis

Two pieces of information are extracted from every measurement. The first one concerns the last stored value of insulation thin film resistance before the breakdown R_0. The second one concerns the early breakdown voltage. The early breakdown voltage is then divided by the critical EBV threshold current 0.2mA thus leading to the EBV resistance estimation, R_{EBV}.

The scatter plots of the measured R_0 for all ageing times and all applied thermal stresses are shown in the following Fig. 4. Black colour stands for measurement 1, blue for consecutive measurement 2 and red for consecutive measurement 3. Firstly, it can be seen that for low ageing times and low thermal stress the diversity between different tested points is stronger than that at longer ageing periods (Fig. 4-a and Fig. 4-b). Moreover, in the same cases (200°C and 215°C) the average resistance of every group is higher always in the third measurement (red colour).

Regarding higher thermal stress (230°C and 245°C) a uniform distribution is observed between the three consecutive measurements in all cases. Moreover, it becomes clear that the average resistances of all cases are significantly lower than those for lower thermal stress (200°C and 215°C). Especially in the last thermal stress case of 245°C, the average resistance is below 500GΩ for all ageing periods and does not significantly vary between them.

Finally, the analysis of the average insulation thin film resistance before the breakdown R_0 reveals that although the increase in temperature decreases the overall average resistance, no monotonic behaviour exists in every thermal stress case along the ageing time (Table II).

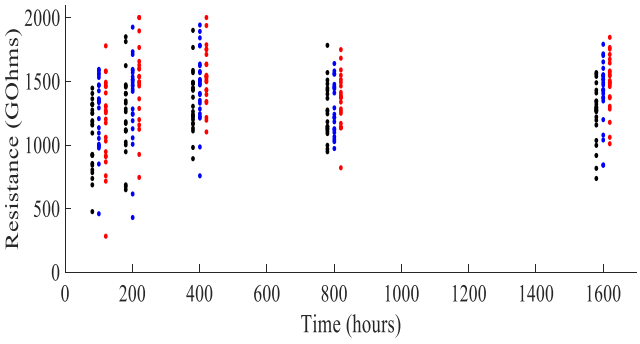

a)

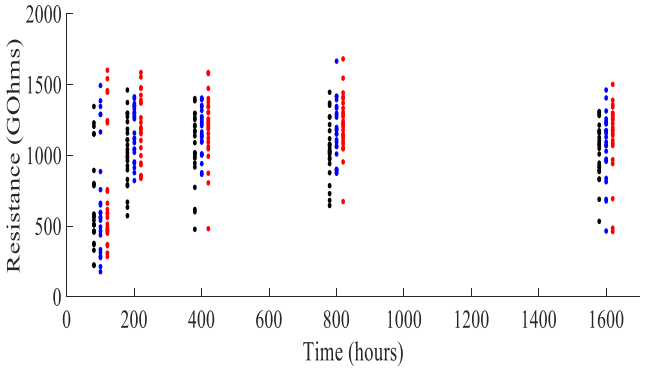

b)

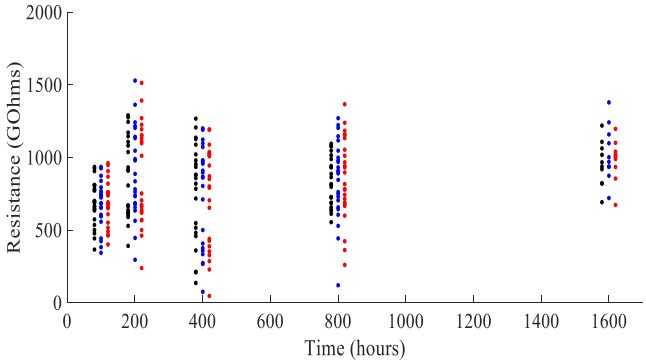

c)

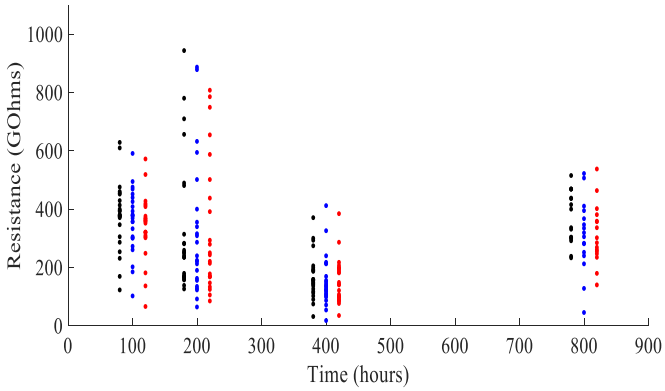

d)

Fig. 4. Scatter plots of the measured R_0 over time for a) 200°C, b) 215°C, c) 230°C and 245°C.

TABLE II. The Average Thin Film Resistance before the Breakdown (GΩ)

	Time (hours)				
Temperature	**100**	**200**	**400**	**800**	**1600**
200°C	1070.14	1240.81	1348.75	1218.01	1251.34
	1249.55	1300.91	1471.09	1240.88	1411.50
	1187.49	1354.20	1535.96	1347.83	1433.31
215°C	669.52	1028.98	1014.87	1049.79	996.20
	699.53	1114.55	1173.35	1170.07	1065.71
	749.62	1137.60	1195.58	1227.49	1131.63
230°C	685.00	841.37	764.15	830.43	956.26
	669.27	884.23	747.99	848.75	1031.11
	688.59	880.75	725.97	856.33	982.52
245°C	378.80	327.14	169.66	371.84	
	359.77	410.64	152.49	309.60	
	339.83	335.00	153.10	313.28	

The maximum values are kept from Table II, and are presented in Fig. 5. It is clear that the resistance drops monotonically with the increase of temperature for each ageing period. However, the drop does not appear to be logarithmic. Moreover, there is not monotonic resistance drop as a function of the ageing time while the thermal stress is fixed.

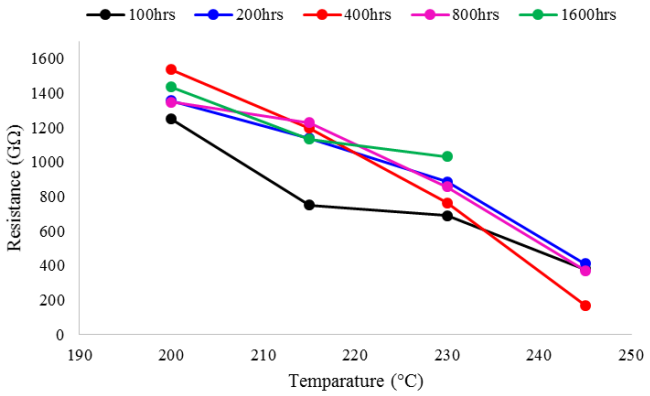

Fig. 5. Dependency of the thin film insulation material maximum resistance before the breakdown on the ageing time and thermal stress.

It was observed that after the third consecutive measurement, the EBV does not significantly vary. For this purpose, the R_{EBV} has been estimated using the EBV from the last consecutive measurement. The results for unaged thin film insulation as well as all studied thermal stresses are shown in the following Fig. 6. The results are presented in the form of Gaussian distributions.

The calculation of the unaged samples' distribution took into account a significant number of measured samples, namely 42. The average resistance is about 49.13MΩ with a standard deviation of 12.51MΩ. The results imply that there is a strong and significant non-uniformity among unaged (healthy) thin film insulation samples.

Furthermore, it can be seen that for 200°C the increase of ageing time shifts the average to the left. Moreover, the standard deviation seems to be the same for 100 hours and 200 hours however it decreases with the increase of the ageing period. Similar observations are made for 215°C. However for the last measurement at 1600 hours, the average seems to be slightly higher than that at 800 hours while the standard deviation increases again. This result is opposing the clear monotonic behaviour of the other studied cases, clearly implying possible critical degradation state.

Additionally, the samples aged at 230°C present a unique pattern. The average breakdown resistance drops from 100 hours to 200 hours as expected with a simultaneous reduction of the standard deviation. However, the resistance slightly increases for 400 hours and drops again for 800 hours. Finally, for 1600 hours the average breakdown resistance is slightly higher than that at 800 hours while the standard deviation is lower. However, the results for 1600 hours are less reliable while some samples of this group were catastrophically damaged during the ageing process.

In the last case of 245°C, there is a small drop of the average breakdown resistance from 100hours to 200hours, however the standard deviation does not change. Longer ageing time leads to further reduction of the breakdown resistance while the standard deviation progressively decreases for 400hours and 800hours.

The results of the early breakdown resistance distributions clearly point out that a simple exponential drop implied by the Arrhenius Law is inadequate to describe the thin film degradation mechanism with accuracy.

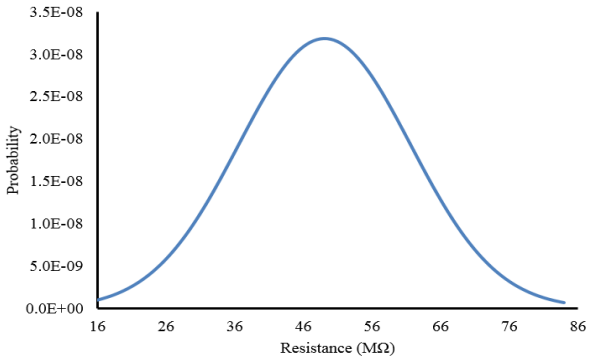

a)

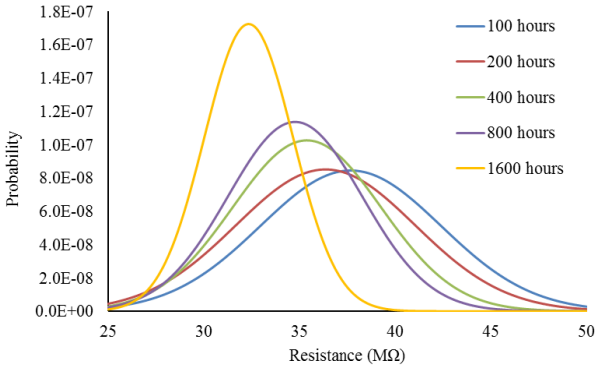

b)

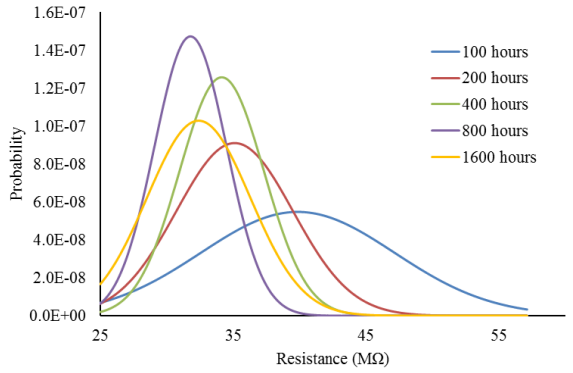

c)

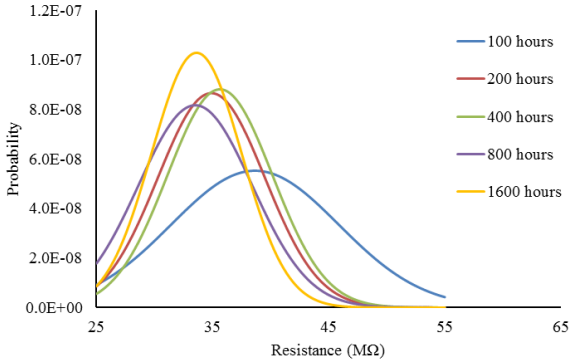

d)

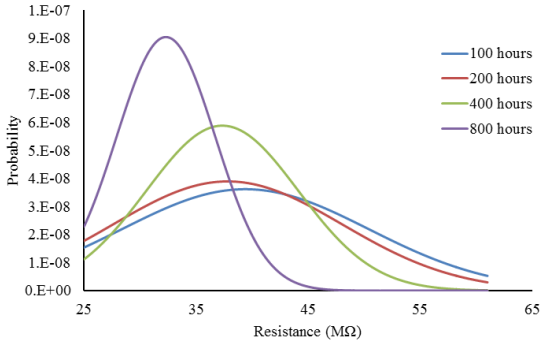

e)

Fig. 6. Normal distributions of the R_EBV for a) unaged material and different ageing periods under b) 200°C, c) 215°C, d) 230°C and e) 245°C thermal stress.

The drop of resistance automatically means higher current through the thin film insulation. To study the dependency of current increase on the applied thermal stress during the breakdown, both resistances before and at early breakdown are required. Writing down Ohm's law before and at the early breakdown, the following equations are given:

$$V_0 = R_0 I_0 \quad (1)$$

$$V_{EBV} = R_{EBV} I_{EBV} \quad (2)$$

However, in this test $V_0 \sim V_{EBV}$. This means that the normalized current increase α is given by:

$$a = \frac{\Delta I}{I_0} = \frac{I_{EBV} - I_0}{I_0} = \frac{R_0 - R_{EBV}}{R_{EBV}} \quad (3)$$

The parameter α is calculated for all tested cases and the results are summarized in the following Fig. 7. The results prove to be satisfying as it is pointed out very clearly that when the thermal stress increases then the breakdown current difference required to break the insulation decreases.

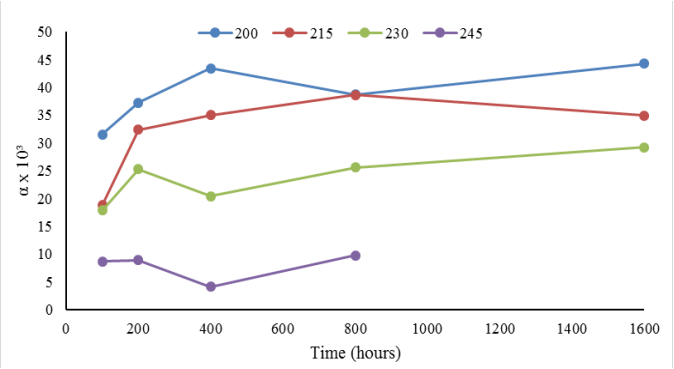

Fig. 7. The dependency of α on the applied stress thermal stress.

IV. Conclusions

This paper describes an experimental procedure which offers insight as to how the thermal degradation of thin film insulation evolves. Experimental results imply that although popular the Arrhenius Law is not capable of describing the full degradation procedure reliably. However, some trends and patterns are observed. It occurs that the thermal degradation leads to the progressive homogenization of the resistive characteristics of the studied thin film insulation material. Interestingly, it seems that the insulation resistance before the EBV does not follow a distinct ageing profile over the ageing time. However, an expected overall drop of the insulation resistance as a function of temperature was recorded. Finally, the normalized current increase has been calculated and a pattern is observed. Specifically, the extra amount of current required to break the insulation is clearly decreases with the thermal stress increase.

References

[1] Y. Fan, C. Li, W. Zhu, X. Zhang, L. Zhang, M. Cheng, "Stator Winding Inter-turn Short Circuit Faults Severity Detection Controlled by OWSVPWM without CMV of Five-phase FTFSCW-IPM", *IEEE Trans. Ind. Appl.*, Vol. 53, No. 1, pp. 194-202, 2017.

[2] A. Ulatowski and A. M. Bazzi, "A Combinational-Logic Method for Electric Vehicle Drivetrain Fault Diagnosis", *IEEE Trans. Ind. Appl.*, Vol. 52, No. 2, pp. 1796-1807, Mar/Apr 2016.

[3] P. J. Tavner, "Review of condition monitoring of rotating electrical machines*", IET Elec. Power Appl.,* Vol. 2, No. 4, pp. 215-247, Jul. 2008.

[4] E. G. Strangas, S. Aviyente, J. D. Neely and S. S. H. Zaidi, "The Effect of Failure Prognosis and Mitigation on the Reliability of Permanent-Magnet AC Motor Drives", *IEEE Trans. Ind. Elec.*, Vol. 60, No. 8, pp. 3519-3528, Aug. 2013.

[5] R. M. Tallam, T. G. Habetler, and R. G. Harley, "Experimental testing of a neural-network-based turn-fault detection scheme for induction machines under accelerated insulation failure conditions," 4th IEEE SDEMPED, pp. 58–62, Stone Mountain, Georgia USA, Aug. 2003.

[6] M. Drif and A. J. M. Cardoso, "Stator Fault Diagnostics in Squirrel Cage Three-Phase Induction Motor Drives Using the Instantaneous Active and Reactive Power Signature Analyses," *IEEE Trans. Ind. Inf*., Vol. 10, No. 2, pp. 1348-1360, May 2014.

[7] N. Lashkari and J. Poshtan, "Detection and discrimination of stator interturn fault and unbalanced supply voltage fault in induction motor using neural network", 6th PEDSTC 201, pp. 275-280, Feb. 2015.

[8] A. Gandhi, T. Corrgan and L. Parsa, "Recent Advances in Modeling and Online Detection of Stator Interturn Faults in Electrical Motors", *IEEE Trans. Ind. Elec*., Vol. 58, No. 5, pp. 1564-1575, 2011.

[9] A. Siddique, G. S. Yadava and B. Singh, "A review of stator fault monitoring techniques of induction motors", *IEEE Trans. Ener. Conv*., Vol. 20, No. 1, pp. 106-114, 2005.

[10] G. C. Stone, E. A. Boulter, I. Culbert, and H. Dhirani, Electrical Insulation for Rotating Machines - Design, Evaluation, Aging, Testing and Repair. IEEE Press Series on Power Engineering, 2004.

[11] K. Younsi, P. Neti, M. Shah, J. Y. Zhou, J. Krahn, and K. Weeber, "Online capacitance and dissipation factor monitoring of ac stator insulation," *IEEE Trans. Dielect. Elect. Insul*., Vol. 17, No. 5, pp. 1441–1452, Oct. 2010.

[12] M. Farahani, E. Gockenbach, H. Borsi, K. Schäfer, and M. Kaufhold, "Behavior of machine insulation systems subjected to accelerated thermal aging test," *IEEE Trans. Dielect. Elect. Insul*., Vol. 17, No. 5, pp. 1364–1372, Oct. 2010.

[13] N. Lahoud, J. Faucher, D. Malec, and P. Maussion, "Electrical aging of the insulation of low-voltage machines: Model definition and test with the design of experiments," *IEEE Trans. Ind. Elect*., Vol. 60, No. 9, pp. 4147–4155, Sep. 2013.

[14] T. M. Wolbank, "On line detection of inverter fed AC machine insulation health state using high frequency voltage excitation", 2015 IEEE ECCE, pp. 4084-4090, 2015.

[15] C. Zoeller, M. A. Vogelsberger and T. M. Wolbank, "Influence of parasitic capacitances of IGBT inverter on insulation condition monitoring of traction machines based on current signal transients analysis", 18th EPE'16 ECCE Europe, Sep. 2016.

[16] C. Zoeller, M. A. Vogelsberger, R. Fasching, W. Grubelnik, and T. M. Wolbank, "Evaluation and current-response based identification of insulation degradation for high utilized electrical machines in railway application," 10th IEEE SDEMPED, Guarda, Portugal, pp. 266–272, Sep. 2015.

[17] M. Sumislawska, O. Agbaje, D. F. Kavanagh and K. J. Burnham, "Equivalent Circuit Model Estimation of Induction Machines under Elevated Temperature Conditions", 2014 UKACC, Loughborough, UK, Jul. 2014.

[18] K. N. Gyftakis, M. Sumislawska, D. F. Kavanagh, D. A. Howey and M. McCulloch, "Dielectric Characteristics of Electric Vehicle Traction Motor Winding Insulation under Thermal Ageing", *IEEE Trans. Ind. Appl*.,Vol. 52, No. 2, pp. 1398-1404, 2016.

[19] M. Sumislawska, K. N. Gyftakis, D. F. Kavanagh, M. McCulloch, K. J. Burnham and D. A. Howey, "The Impact of Thermal Degradation on Properties of Electrical Machine Winding Insulation Material", *IEEE Trans. Ind. Appl.*, Vol. 52, No. 4, pp. 2951-2960, 2016.

[20] F. Salameh, A. Picot, M. Chabert, E. Leconte, A. Ruiz-Gazen and P. Maussion, "Variable importance assessment in lifespan models of insulation materials: A comparative study", 2015 IEEE 10th SDEMPED, Guarda, Portugal, Sep. 2015.

[21] Arrhenius, S.A., "Über die Dissociationswärme und den Einfluß der Temperatur auf den Dissociationsgrad der Elektrolyte". Z. Phys. Chem. 4: 96–116, 1889.

[22] Arrhenius, S.A., "Über die Reaktionsgeschwindigkeit bei der Inversion von Rohrzucker durch Säuren". ibid. 4: 226–248, 1889.